Rakenteiden Mekaniikka (Journal of Structural Mechanics)
Vol. 48, No 3, 2015, pp. 164 – 180
rmseura.tkk.fi/rmlehti/

VERTAISARVIOITU
KOLLEGIALT GRANSKAD
PEER-REVIEWED
www.tsv.fi/tunnus

Differential cubature method for gradient-elastic Kirchhoff plates

S. Mahmoud Mousavi[1], Jarkko Niiranen, Antti H. Niemi

Summary. In this article, the differential cubature method is applied for the problem describing the static deformations of gradient-elastic Kirchhoff plates. The theory of gradient elasticity applied for the Kirchhoff plate model results in a sixth order partial differential equation with a set of corresponding boundary conditions. The differential cubature method is shown to be able to solve the problem with a relatively small number of grid points and with a small computational effort. In particular, the correct qualitative dependence of the solution on the size effect parameter is encountered. However, it is demonstrated that the differential cubature method possesses certain deficiencies related to the resulting system matrices and enforcement of boundary conditions, which is an issue that, surprisingly, has not been studied thoroughly before.

Key words: strain gradient elasticity, size effect, Kirchhoff plate, differential cubature method, boundary conditions

Received 30 April 2015. Accepted 13 December 2015. Published online 18 December 2015.

Introduction

Plates are very common structures in many applications in different fields of science and technology, especially in civil and mechanical engineering. For the sake of simplicity and efficiency, plate structures are usually modelled by dimension reduction, i.e., the 3D structure is approximately modelled by a 2D model with the thickness appearing as a parameter in the model.

Within this approach, the most commonly used models for plate structures in engineering applications are the Reissner–Mindlin and Kirchhoff–Love plate models [13, 17], the former being capable of modelling a wide range of applications of moderately thick plate structures, various options for loadings and different types of boundary conditions as well [15, 4, 41]. In particular, the Reissner–Mindlin model can be regarded as the lowest-order member of a more general class, the hierarchical plate models of dimension reduction [32, 31].

Within the classical elasticity theory, the Kirchhoff plate model leads to a fourth order partial differential equation – the biharmonic equation in the simplest cases. During the past decades, different computational methods have been successfully applied for the

[1]Corresponding author. mahmoud.mousavi@aalto.fi

classical Kirchhoff plate problems with various boundary conditions – the main focus being placed on finite element methods (FEM), cf. [5, 25, 16, 6, 18, 8, 9, 7]. The primary challenge in designing appropriate finite element methods for the Kirchhoff plate problem has been related to the fundamental fact that the differential equation of the problem is of fourth order, which implies an H^2 setting for the weak formulation requiring either C^1 continuity from the approximation functions for conforming methods or, alternatively, a nonconforming approach.

The classical elasticity theory has been shown to be incapable of describing size dependent, but still elastic, phenomena of structures which have been, however, observed experimentally for metals and polymers, see for instance [20, 24]. Generalized continuum theories, instead, include length scale parameters for taking into account the size effects possibly present in structures. For instance, in the strain gradient elasticity theory, the strain energy is generalized such that it is not simply a function of the strain but also depends on the gradient of the strain (multiplied by a length scale parameter). The generalized continuum elasticity theories were introduced at the beginning of the nineteenth century first by the Cosserat brothers. About half a century later, these theories were revised by the founders of modern continuum mechanics (Toupin, Rivlin, Mindlin, Eringen and others) as reviewed by Altenbach et al. [3].

Regarding gradient-elastic Kirchhoff plates, in [10] a sixth order governing equation has been derived by using the strong form of the equilibrium equations. As expected, this approach provides no information about the corresponding new boundary conditions. However, in [11] a variational approach for the same problem has been presented implying the governing equation as well as a set of boundary conditions. In [21] the governing plate equation and the corresponding boundary conditions have been derived via a variational method as well. Another type of Kirchhoff plate model based on a modified couple stress theory has been presented in [35, 38]. However, the resulting boundary value problem is of the fourth order as the classical plate equation. All of these formulations for gradient-elastic Kirchhoff plates consider only one material length scale parameter. In [37], instead, a Kirchhoff micro-plate model based on the strain gradient elasticity theory have been developed providing three material length scale parameters to capture the size effects. The problem has been solved for simply supported boundary conditions in [11]. Furthermore, another Kirchhoff micro-plate model based on the modified strain gradient elasticity theory have been presented in [30]. The formulation is quite general and can be reduced to the modified couple stress plate model or to the classical plate model once two or all material length scale parameters are set zero, respectively.

Regarding numerical methods, some non-standard methods have been extended to the problems of gradient elasticity in recent years. This can be regarded natural – and even desirable – since a conforming finite element methods which, at the first glance, could be considered as a practical mainstream approach, would lead to nonstandard approaches. In the territory of Kirchhoff micro-plates, especially, for the sixth order partial differential equation an H^3 regular weak formulation implies the requirement of nonstandard C^2 continuous higher order piecewise polynomial basis functions. This type of a higher continuity finite element method has been used in [1] for the static deflection analysis of a rectangular micro-plate, while in [2] the static deflection analysis of a simply supported sectorial micro-plate using a p-version finite element method have been presented. The boundary element method (BEM) has also been shown to be applicable for the static and dynamic analysis of strain gradient-elastic solids and structures [36, 34].

For the dynamic analysis of structures, one might need to take into account velocity

gradient as well as strain gradient. Higher-order shear deformable beam and plate within strain and velocity gradients theory is studied in [29] and [40], respectively. In these papers, a variational approach is followed and the motion equations and the consistent boundary conditions of gradient theory are derived for shear deformable beam and plate.

The differential cubature method (DCM) applied in the present contribution has been introduced in [14] as an efficient procedure to obtain solutions for partial differential equations with a relatively small number of grid points and small computational effort. In the literature, DCM has been applied for plate problems of classical elasticity, i.e., for the fourth order problems, including bending [22, 23, 33] and vibration [39]. Furthermore, it has been applied to the bending analysis of laminated cylindrical panels [27], and to the statics of laminated shells of revolution with mixed boundary conditions [26].

In the present article, in the following section, DCM is applied for solving the problem of Kirchhoff micro-plates governed by a sixth order partial differential equation with the corresponding boundary conditions which have been derived by a variational approach of gradient elasticity in [11]. Next, the differential cubature method and its main features are explained briefly. Then a set of numerical results is presented. Finally, the main conclusions are outlined.

Governing equations and boundary conditions for gradient-elastic Kirchhoff plates

Adopting Kirchhoff's theory of plates, a flat thin plate can be described by its mid-surface Ω in the (x, y) plane and the thickness $t << \text{diam}(\Omega)$. A lateral static load $q = q(x, y)$ is idealized to be distributed on the mid-surface of the plate resulting in a lateral deflection $w = w(x, y)$ in the z direction.

For simplicity, the plate is assumed to be isotropic with constant thickness t and modulus of elasticity, E, and Poisson's ratio, ν. The micro-structural effects of the material are expressed by the characteristic length g. Furthermore, the classical flexural plate rigidity, or bending stiffness, is defined as

$$D = \frac{Et^3}{12(1-\nu^2)}. \tag{1}$$

Similar to the classical Kirchhoff plate elasticity, the variational approach applied to the Kirchhoff micro-plate elasticity results in a formulation consisting of governing partial differential equation and boundary conditions. In [11, 10], the governing equation of the problem has been derived in the form

$$D\nabla^4 w - g^2 D\nabla^6 w = q \quad \text{in } \Omega, \tag{2}$$

with the partial differential operators defined in a standard way as

$$\nabla^4 = \frac{\partial^4}{\partial x^4} + \frac{\partial^4}{\partial y^4} + 2\frac{\partial^4}{\partial x^2 \partial y^2} \tag{3}$$

$$\nabla^6 = \frac{\partial^6}{\partial x^6} + \frac{\partial^6}{\partial y^6} + 3\frac{\partial^6}{\partial x^4 \partial y^2} + 3\frac{\partial^6}{\partial y^4 \partial x^2}. \tag{4}$$

There are slightly different forms of the governing equation for first-order gradient-elastic Kirchhoff plates due to different constitutive equations such as those in [11] and

[28]. In the current model, the bending moments and the twisting moments are defined as

$$M_x = -D\big(\frac{\partial^2 w}{\partial x^2} + \nu\frac{\partial^2 w}{\partial y^2}\big) + g^2 D\big(\frac{\partial^4 w}{\partial x^4} + \nu\frac{\partial^4 w}{\partial y^4} + (1+\nu)\frac{\partial^4 w}{\partial x^2 \partial y^2}\big), \tag{5}$$

$$M_y = -D\big(\frac{\partial^2 w}{\partial y^2} + \nu\frac{\partial^2 w}{\partial x^2}\big) + g^2 D\big(\frac{\partial^4 w}{\partial y^4} + \nu\frac{\partial^4 w}{\partial x^4} + (1+\nu)\frac{\partial^4 w}{\partial x^2 \partial y^2}\big), \tag{6}$$

$$M_{xy} = -D(1-\nu)\frac{\partial^2 w}{\partial x \partial y} + g^2 D(1-\nu)\big(\frac{\partial^4 w}{\partial x^3 \partial y} + \frac{\partial^4 w}{\partial y^3 \partial x}\big), \tag{7}$$

while the shear forces are defined through the moment balance as usual:

$$Q_x = \frac{\partial M_x}{\partial x} + \frac{\partial M_{xy}}{\partial y}, \quad Q_y = \frac{\partial M_y}{\partial y} + \frac{\partial M_{xy}}{\partial x}. \tag{8}$$

Boundary conditions of the problem will be discussed in context of the numerical results in the following sections.

Differential cubature method in brief

In this section, we recall the basics of the differential cubature method and point out the main advantages and disadvantages of the method from the theoretical point of view.

According to differential cubature method, any linear operation such as a continuous function or various orders of partial derivatives of a multivariate function can be expressed as a weighted linear sum of discrete functions chosen within the overall domain of the problem [14]. For instance, in a two-dimensional problem, the cubature approximation of a linear differential operator L (representing of an operator of any order of partial derivatives or combinations of these partial derivatives) of function $f(x, y)$ at the node i is given by

$$\big(L\{f(x,y)\}\big)_i = \sum_{j=1}^{n} c_{ij} f(x_j, y_j), \quad i = 1, ..., n \tag{9}$$

where i is the index of arbitrarily sequenced grid points for the two-dimensional solution domain, n is the total number of discrete points within the domain and c_{ij} are the unknown cubature weighting coefficients which for n grid points constitute n^2 unknowns to be determined.

In order to determine these coefficients, a set of monomial basis functions

$$F(x, y) = x^{m-n} y^n, \quad m = 0, 1, 2, ..., k-1, \quad n = 0, 1, 2, ..., m \tag{10}$$

are often used. Other type of basis functions like harmonic functions or Bessel functions have been proposed in [12], for instance. The basis functions in Eqs. (10) are taken from the "Pascal triangle of monomials" in x and y with m referring to the row index of the "Pascal triangle". For instance, monomials up to level $m = 2$ are simply 1 ($m = 0$), x, y ($m = 1$), x^2, xy, y^2 ($m = 2$).

The number of monomials should be equal to the number of total grid points n. Therefore, the appropriate value of k in Eqs. (10) has to be be determined in order to satisfy this condition. For instance, for the case with $n = 41$, all of the monomials up to $m = 8$ should be used giving only $m(m+1)/2 = 36$ monomials. Therefore, five more monomials from the level $m = 9$ should be selected to provide 41 monomials. It has been

found out that the method of the selection of these five additional monomials from the next line ($m = 9$) has insignificant effect on the solution.

Once the set of monomials is constructed, the monomials are substituted into Eqs. (9) in order to construct n equations. Moreover, introducing the obtained n equations to all n grid points leads to the following set of n^2 equations composed of $n \times n$ real matrices for determining the n^2 unknowns c_{ij}:

$$\begin{pmatrix} \left(L\{f_1\}\right)_1 & \left(L\{f_2\}\right)_1 & \cdots & \left(L\{f_n\}\right)_1 \\ \left(L\{f_1\}\right)_2 & \left(L\{f_2\}\right)_2 & \cdots & \left(L\{f_n\}\right)_2 \\ \vdots & \vdots & \ddots & \vdots \\ \left(L\{f_1\}\right)_n & \left(L\{f_2\}\right)_n & \cdots & \left(L\{f_n\}\right)_n \end{pmatrix}$$
$$= \begin{pmatrix} c_{11} & c_{12} & \cdots & c_{1n} \\ c_{21} & c_{22} & \cdots & c_{2n} \\ \vdots & \vdots & \ddots & \vdots \\ c_{n1} & c_{n2} & \cdots & c_{nn} \end{pmatrix} \begin{pmatrix} f_1(x_1, y_1) & f_2(x_1, y_1) & \cdots & f_n(x_1, y_1) \\ f_1(x_2, y_2) & f_2(x_2, y_2) & \cdots & f_n(x_2, y_2) \\ \vdots & \vdots & \ddots & \vdots \\ f_1(x_n, y_n) & f_2(x_n, y_n) & \cdots & f_n(x_n, y_n) \end{pmatrix} \tag{11}$$

This process should be accomplished for all of the operators in the governing equations and possible boundary conditions.

Having determined all the coefficients for each differential operator appearing in the governing equations, one substitutes them according to Eqs. (9) into the governing equation (2) to reach a set of n linear algebraic equations. Finally, the same procedure is applied to all boundary conditions. It should be noted that this procedure yields an over-determined system of equations with system matrix B. The number of equations can be reduced by not imposing the governing equation at the grid points lying on the boundary. Indeed, since the governing equations are valid only in the interior part of the domain and the boundary conditions are valid on the boundaries of the domain, the grid points for enforcing the governing equations should not include any boundary points. In any case, for higher-order problems as Kirchhoff plates, the system remains over-determined. In order to overcome this problem, the least squares method is used to solve the final system in the current approach as is common in context of DCM. Regarding solution procedures of the resulting linear system, it should be noted that the matrices above are full matrices, which can be seen as a drawback of the method.

The differential cubature method involves a penalty parameter which controls the relative weight of the boundary conditions in the final system of algebraic equations. The penalization is done by multiplying the relevant line of the boundary equations to the parameter. This coefficient ensures the satisfaction of the relevant boundary conditions. The theoretical study of the DCM and its error analysis incorporating the penalization parameter is excluded from the current analysis. Instead, we study the sensitivity of the method with respect to this parameter in the next section by numerical means.

In DCM, the plate domain is to be covered by several grid points, and a particular procedure should be used for node generation and their numbering [27]. The relevance of this issue has been pointed out also in [14] although no rigorous theoretical analysis for this issue seems to exist and even no numerical demonstrations illustrating the sensibility of the method on the grid point positioning. According to [19], "the conventional rectangular grid systems with equally spaced grid points used frequently with the quadrature and finite difference methods lead to a singularity problem in the solution". The reason for this seems to be an ill-conditioned Vandermonde type system matrix, cf. [14]. In addition,

[12] propose using roots of Chebyshev, Gauss, or Legendre polynomials as the grid spacing approaches that has been applied for quadrature methods, for instance.

As a part of numerical results in the following sections, we have demonstrated how the condition number of the system matrix and the convergence of the solution depend on the positioning of the grid points. In order to analyze the DCM for plates with different geometries, we have used circular and rectangular plates as examples. For more general geometries, however, it is sufficient to distribute the nodal points randomly in the plate mid-plane and on its boundary, as explained here and also reported in other related articles as in [22]. For a rectangular plate, the grid points are chosen first as a set of uniform rectangular grid with small random deviations, second as a set of uniform diamond shaped grid, cf. [27, 23] (see an example distribution of 41 nodal points in Fig. 1). An example of a 25 nodal points distribution of a circular plate is demonstrated in Fig. 2.

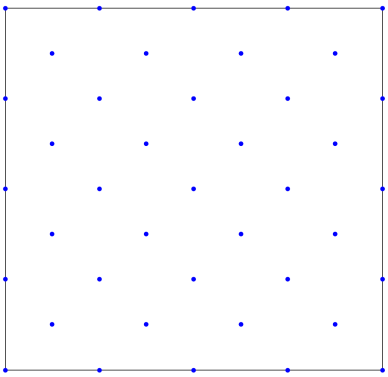

Figure 1. A distribution of 41 grid points for a rectangular plate.

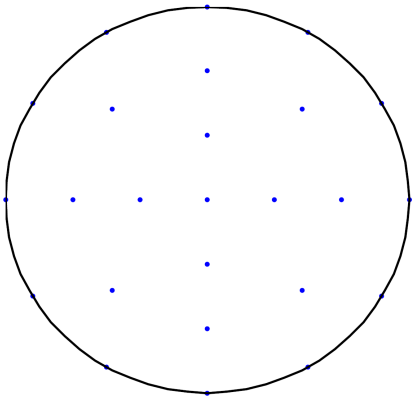

Figure 2. A distribution of 25 grid points for a circular plate.

Numerical results

This section is dedicated for applying the differential cubature method for two types of benchmark problems of gradient-elastic Kirchhoff plates – a rectangular plate with simply supported and clamped boundaries; a circular plate with clamped boundaries – for addressing the applicability and generality of the method with respect to plate geometries and boundary conditions, in particular. Furthermore, the convergence properties of the method as well as the sensitivity of the method with respect to the grid positioning and penalty coefficient for boundary conditions is studied thoroughly.

A rectangular plate with clamped and simply supported boundaries

Let us here consider a rectangular plate with side lengths a and b. An analytic reference solution for a rectangular gradient-elastic plate, simply supported at all boundaries (SSSS) can be derived as follows. Under a sinusoidal loading

$$q(x,y) = q_0 \sin\frac{\pi x}{a}\sin\frac{\pi y}{b} \tag{12}$$

the plate deflection takes the form (cf. the classical Navier solution and [10])

$$w(x,y) = \frac{q_0}{\pi^4 D\Big(1+\big(1+(a/b)^2\big)\pi^2(g/a)^2\Big)(1/a^2+1/b^2)^2}\sin\frac{\pi x}{a}\sin\frac{\pi y}{b} \tag{13}$$

giving the central deflection

$$w_0 = \frac{q_0}{\pi^4 D\Big(1 + \big(1 + (a/b)^2\big)\pi^2 (g/a)^2\Big)(1/a^2 + 1/b^2)^2} \tag{14}$$

which can be compared to the central deflection of the corresponding classical Navier solution at $g = 0$ of the form

$$w_{0,cl} = \frac{q_0}{\pi^4 D(1/a^2 + 1/b^2)^2}. \tag{15}$$

The procedure explained in the previous section for the DCM is applied for this problem and the numerical results of DCM are compared with the reference solution (13) and also with those obtained by C^2 continuous finite element methods, see [1]. The specific form of boundary conditions used in these references is

$$\begin{aligned} w = \frac{\partial^2 w}{\partial x^2} = \frac{\partial^2 w}{\partial y^2} = \frac{\partial^4 w}{\partial x^4} = \frac{\partial^4 w}{\partial y^4} = \frac{\partial^4 w}{\partial x^2 \partial y^2} = 0 \quad \text{at} \quad x = 0, a \\ w = \frac{\partial^2 w}{\partial y^2} = \frac{\partial^2 w}{\partial x^2} = \frac{\partial^4 w}{\partial y^4} = \frac{\partial^4 w}{\partial x^4} = \frac{\partial^4 w}{\partial y^2 \partial x^2} = 0 \quad \text{at} \quad y = 0, b. \end{aligned} \tag{16}$$

One should notice that these boundary conditions lead to satisfaction of the conditions

$$\begin{aligned} w = M_x = 0 \quad \text{at} \quad x = 0, a \\ w = M_y = 0 \quad \text{at} \quad y = 0, b \end{aligned} \tag{17}$$

representing the classical simply supported boundary conditions in terms of the moments (Eqs. 5 and 6). Regarding the additional non-classical boundary conditions, there are two options, namely either

$$\begin{aligned} \frac{\partial^2 w}{\partial x^2} = 0 \quad \text{at} \quad x = 0, a \\ \frac{\partial^2 w}{\partial y^2} = 0 \quad \text{at} \quad y = 0, b \end{aligned} \tag{18}$$

or

$$\begin{aligned} -g^2 D \left(\frac{\partial^3 w}{\partial x^3} + \nu \frac{\partial^3 w}{\partial x \partial y^2} \right) = 0 \quad \text{at} \quad x = 0, a \\ -g^2 D \left(\frac{\partial^3 w}{\partial y^3} + \nu \frac{\partial^3 w}{\partial y \partial x^2} \right) = 0 \quad \text{at} \quad y = 0, b. \end{aligned} \tag{19}$$

These boundary conditions have been derived using the variational approach in [11]. Notice that, the form (16) corresponds to Eq. (18) and is satisfied by the reference solution (13) while that solution does not satisfy Eq. (19). However, both forms of additional boundary conditions can be enforced in the cubature method.

First, we compare DCM with the reference solution (13) and the corresponding finite element solution of [1] using the boundary conditions (17) and (18) or (19). Fig. 3 depicts the normalized central deflection versus the square of the dimensionless length scale parameter $(g/a)^2$ for the different methods. The other problem parameters are taken to be $\nu = 0.3$, $b/a = 1$ and $t/a = 0.1$. E is used for normalizing the loading by setting $q_0 = E$. The DCM solution is obtained using $n = 85$ grid points in the diamond formation. Other type of spacing of the grid points is studied in Table 1.

Table 1. Condition number and convergence for different grid point positionings at $g/a = 0.1, \lambda = 1e4$ (rectangular plate).

Grid points	Condition number	Midpoint deflection	Midpoint moment
		$w = 2.9255$	$M_x = 2.9354e+04$
N	$\kappa(B)$	$w(a/2, b/2)$	$M_x(a/2, b/2)$
Diamond shaped grid			
41	$2.7689e+18$	3.4132	$3.6669e+04$
61	$3.7004e+19$	2.8956	$3.3010e+04$
85	$6.5243e+20$	2.9265	$3.2932e+04$
113	$4.0816e+20$	2.9258	$3.2929e+04$
145	$3.2387e+20$	2.9232	$3.2924e+04$
181	$3.3506e+22$	diverge	diverge
Random nodes			
25	$4.7410e+18$	5.3319	$5.9192e+04$
49	$1.9902e+18$	3.3367	$3.4633e+04$
81	$5.1226e+18$	2.9200	$3.2905e+04$
121	$1.2477e+19$	2.9245	$3.2931e+04$
169	$6.1750e+18$	diverge	diverge

A penalty coefficient is employed to impose the boundary conditions. It is observed that, with penalty coefficient $\lambda = 1e4$ (or higher, not reported here), the DCM solution is almost identical to the analytical reference solution and close to the FE solution. For the latter, there is no detailed information about the discretization such as the mesh spacing in [1]. With $\lambda = 1e2$ (or lower, not reported here), there is a slight deviation from the exact solution.

Second, we study the effect of the non-classical boundary conditions to the micro-plate deflection. Fig. 4 depicts again the normalized central deflection versus the square of the dimensionless length scale parameter $(g/a)^2$ for the two different boundary conditions (18) (Type 1) and (19) (Type 2). The DCM solution has been obtained by using the same problem and discretization parameters as before. According to these results, for the boundary condition (19), DCM results converge by increasing λ for gradient parameter higher than $g = 0.1a$, while for smaller values of g the results become highly dependent on the value of the penalty parameter λ.

In what follows, we will study the sensitivity of DCM to the discretization parameters, namely the number of grid points n and the penalty parameter λ. For this purpose we use the boundary conditions of Type 1 corresponding to the analytical solution (13). The convergence results of DCM with respect to the number of grid points n are shown in Fig. 5 for the normalized central deflection along the line $x = a/2$ for $g/a = 0.1$. Other problem and discretization parameters are the same as before. It can be concluded that for the value $n = 41$ the deflection is higher than the exact solution. For parameter values $n = 61, 85, 113$, the numerical solution is very close to the exact solution. However, further increasing of n breaks the method down. This can be seen in Table 1 demonstrating the convergence of the midpoint deflection $w(a/2, b/2)$ and the moment $M_x(a/2, b/2)$ as well as the condition number of the system matrix for two different positioning of the grid points. Here we take $g/a = 0.1$ while the other discretization parameters are

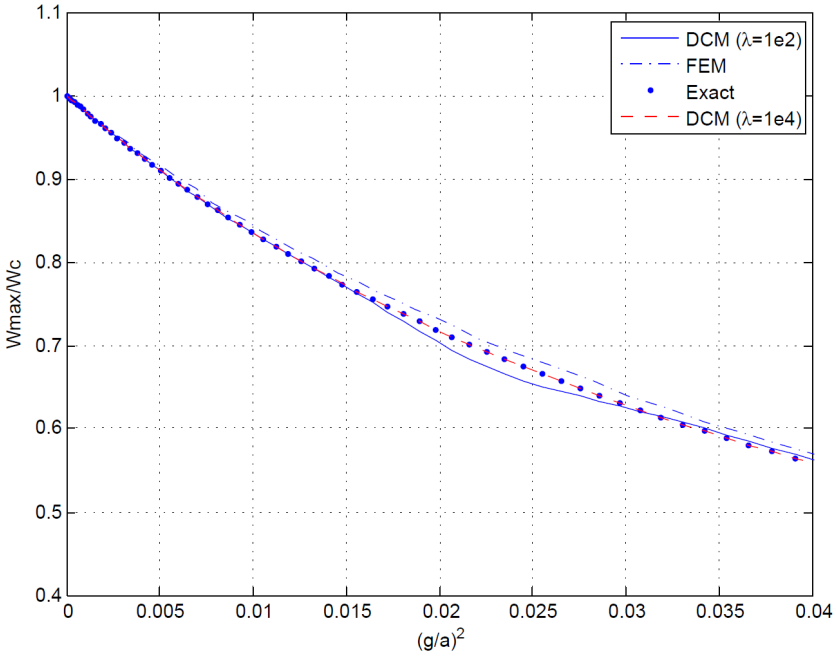

Figure 3. The normalized central deflection versus dimensionless length scale parameter for a simply supported micro-plate using the boundary conditions (16), $n = 85$.

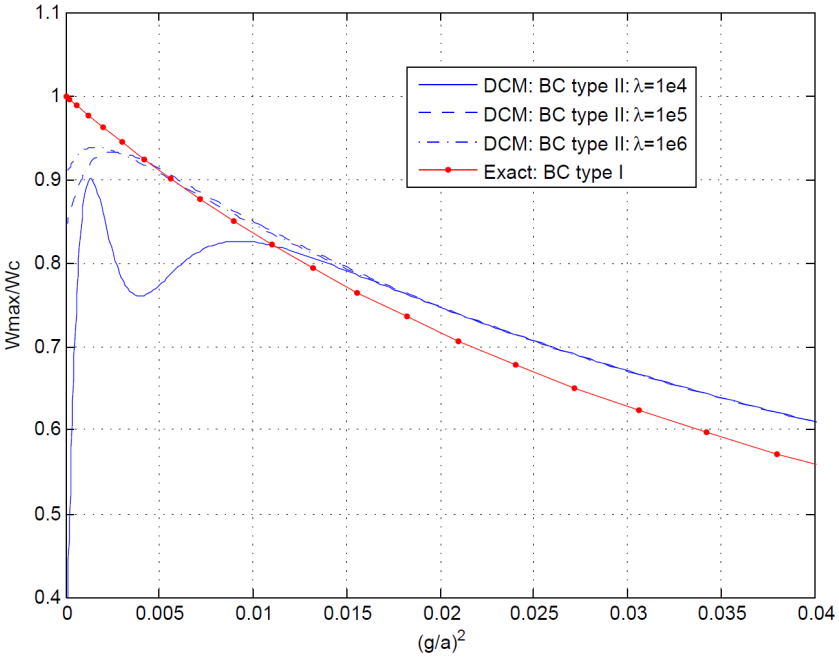

Figure 4. The normalized central deflection versus dimensionless length scale parameter for a simply supported micro-plate using the boundary conditions (17) and (19), $n = 85$.

once again the same as before. Considering the exact solution ($w(a/2, a/2) = 2.9255$, $M_x(a/2, a/2) = 2.9354e+04$), it is observed that the diamond shaped grid point provides results with less errors than random nodes for both the deflection and the moment of the plate. The random nodes are created by applying random deviations to a uniform grid.

Table 2 represents similar results for $g/a = 0$. In this case, the same observations and conclusions regarding the grid points and their positioning remain valid.

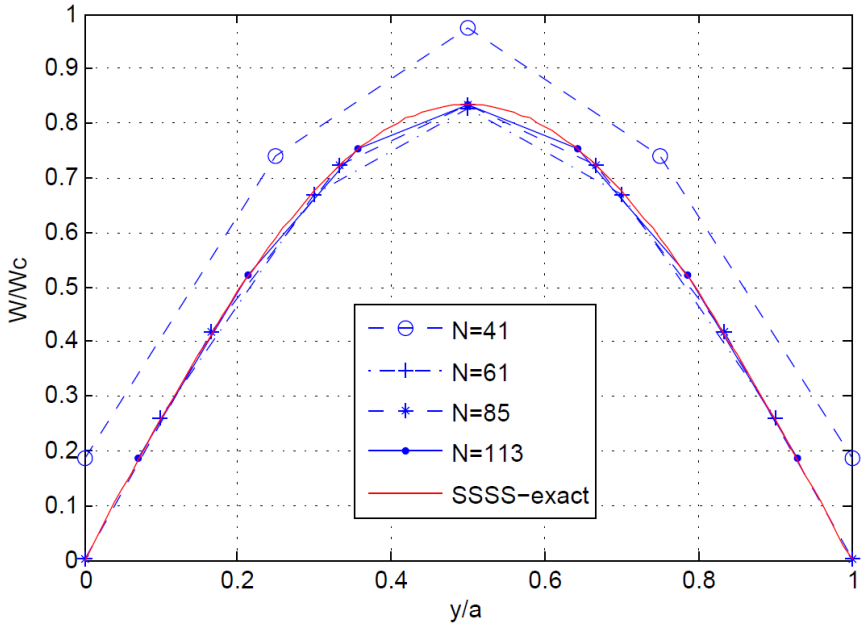

Figure 5. Convergence of DCM in the case of a simply supported plate (SSSS). BC Type 1. $\lambda = 1e4$ and $g = 0.1a$

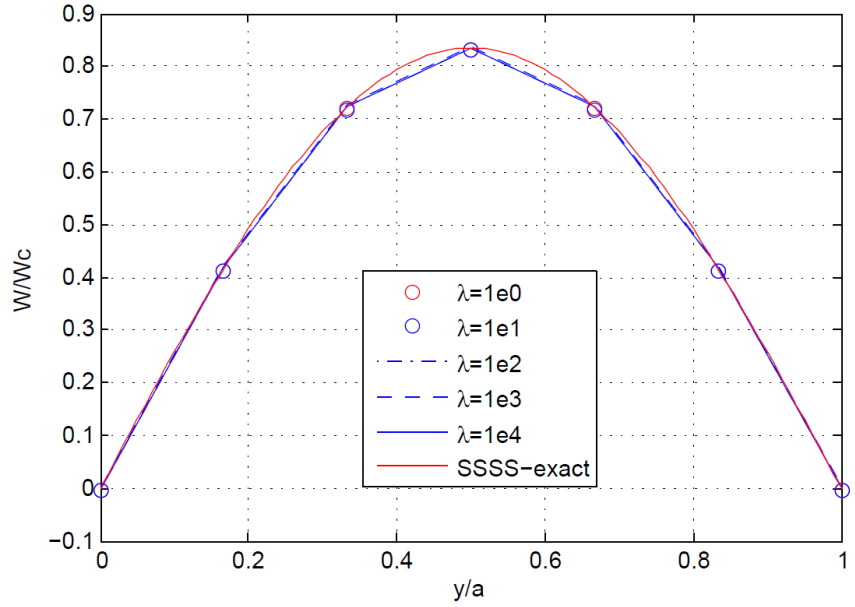

Figure 6. Effect of the penalty coefficient (λ) on plate deflection in the case of a simply supported plate (SSSS). $g = 0.1a$ and $n = 85$.

For a simply supported plate, the effect of the penalty parameter λ on plate deflection is demonstrated in Fig. 6 and Fig. 7 for $g = 0.1a$ and $g = 0.15a$, respectively. In these figures, the number of the grid points is $n = 85$. In this case the method seems not very sensitive to the magnitude of the penalty parameter over the range $\lambda \in [10^4, 10^8]$.

Substitution of the Eq. (13) in Eqs. (5), (6), (7) and (8) results in the analytical solutions for the moments and shear forces. Moments and shear forces corresponding to the DCM method are obtained by calculating the cubature weights corresponding to

Table 2. Condition number and convergence for different grid point positionings at $g/a = 0, \lambda = 1e4$ (rectangular plate).

Grid points N	Condition number $\kappa(B)$	Midpoint deflection $w = 3.5033$ $w(a/2, b/2)$	Midpoint moment $M_x = 3.2929e+04$ $M_x(a/2, b/2)$
Diamond shaped grid			
41	$2.3480e+19$	3.4975	$3.2902e+04$
61	$5.8333e+18$	3.5032	$3.2918e+04$
85	$8.6314e+19$	3.5033	$3.2929e+04$
113	$1.4813e+19$	3.5033	$3.2930e+04$
145	$3.3130e+18$	3.4991	$3.2918e+04$
181	$5.0881e+18$	diverge	diverge
Random nodes			
25	$2.1113e+19$	5.7725	$4.8332e+04$
49	$2.2085e+18$	3.5022	$3.2914e+04$
81	$2.0000e+18$	3.5044	$3.2934e+04$
121	$3.8344e+17$	diverge	diverge

Eqs. (5), (6), (7) and (8). The results for the deflection obtained via DCM are used to produce grid data by cubic interpolation for visualization. Fig. 8 compares the numerical and analytical results for the moment component M_x. The number of grid points is $n = 85$ for the numerical solutions. These results are in good agreement.

Finally, for curiosity, some results for another boundary condition type is presented. In this case, all the boundaries are assumed to be clamped (CCCC). The nonclassical boundary condition is considered to be given by Eq. (18). In Fig. 9, the normalized central deflection versus gradient parameter is drawn for the cases of SSSS, CCCC. It should be mentioned that the deflections are normalized with the deflection of the simply supported classical plate. Again, DCM results converge by increasing λ for gradient parameter higher than $g = 0.1a$, while for smaller values of g the results become highly dependent on the value of the penalty parameter λ.

A circular plate with clamped boundaries

Let us consider a circular plate with clamped boundaries. In the case of uniform loading q_0, the analytical solution is given in [11]. This reference solution is derived by considering the first option of the nonclassical boundary condition,

$$\frac{\partial^2 w}{\partial n^2} = 0 \quad \text{at} \quad r = a. \tag{20}$$

In Fig. 10, for gradient parameter $g = 0.1a$, with a denoting the radius of the plate, the results obtained by using DCM (with $\lambda = 1e4$) are compared to the analytical solution. The convergence of the radial deflection regarding to the number of grid points can be observed. For $N = 113$, the DCM predication has converged very close to the analytical solution.

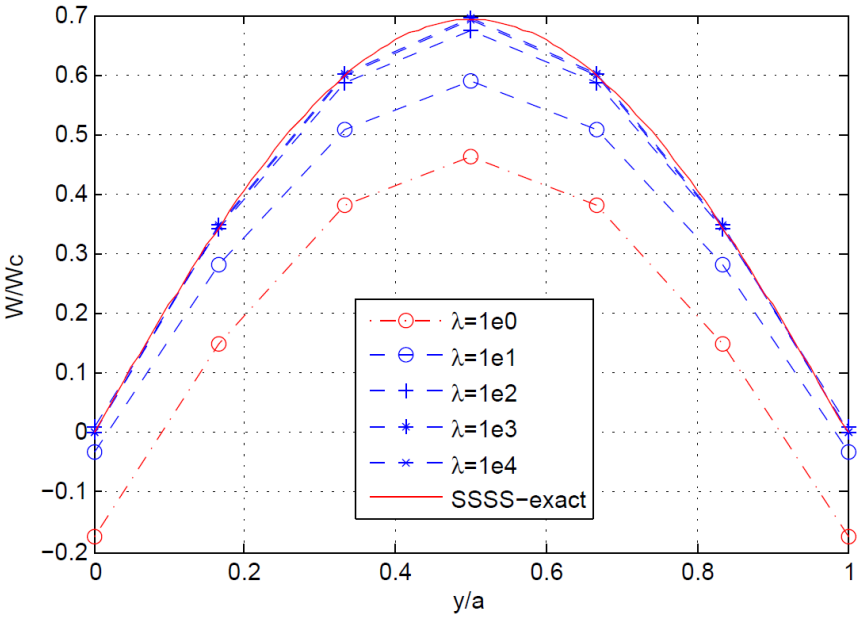

Figure 7. Effect of the penalty coefficient (λ) on plate deflection in the case of a simply supported plate (SSSS). $g = 0.15a$ and $n = 85$.

Conclusions

In the present work, differential cubature method (DCM) has been applied to analyse the statics of gradient-elastic Kirchhoff plates. In the gradient elasticity theory adopted in the present work, the characteristic length scale of the micro-plate is taken into account by one gradient parameter. Increasing the value of the gradient parameter results in decreasing values for the deflection of the plate when compared to the corresponding classical plate model.

The results obtained by DCM for approximating the deflection of a simply supported rectangular Kirchhoff micro-plate benchmark problem depicts very good agreement with the reference solutions provided that the discretization parameters are carefully chosen. The same holds true for the clamped circular plate. The differential cubature method is capable of analysing plates with arbitrary geometries.

The main generic problems of the method found here, which have not been studied thoroughly before, seems to be the requirement of specific grid positioning and the divergence of the solution for high but still modest number of grid points. Also specification of the value of the penalty coefficient enforcing the boundary conditions presents difficulties in some cases, especially for small values of the length scale parameter in the present problem. In addition, the condition number of the system matrix (B) is very high in the example cases, which should be considered as an alarming drawback of the method although standard solvers have been successfully used in the computations of the current examples.

The results demonstrate the capability of the method for considering Type 1 boundary conditions of gradient elasticity (18), while numerical accuracy issues are encountered for the Type 2 boundary conditions (19). It seems that the parameter-dependence of the current gradient elasticity problem, especially in the context of the higher-order boundary conditions, is the reason for the numerical problems observed. These observations indicate that the parameter dependence specific to problems in gradient elasticity, in gen-

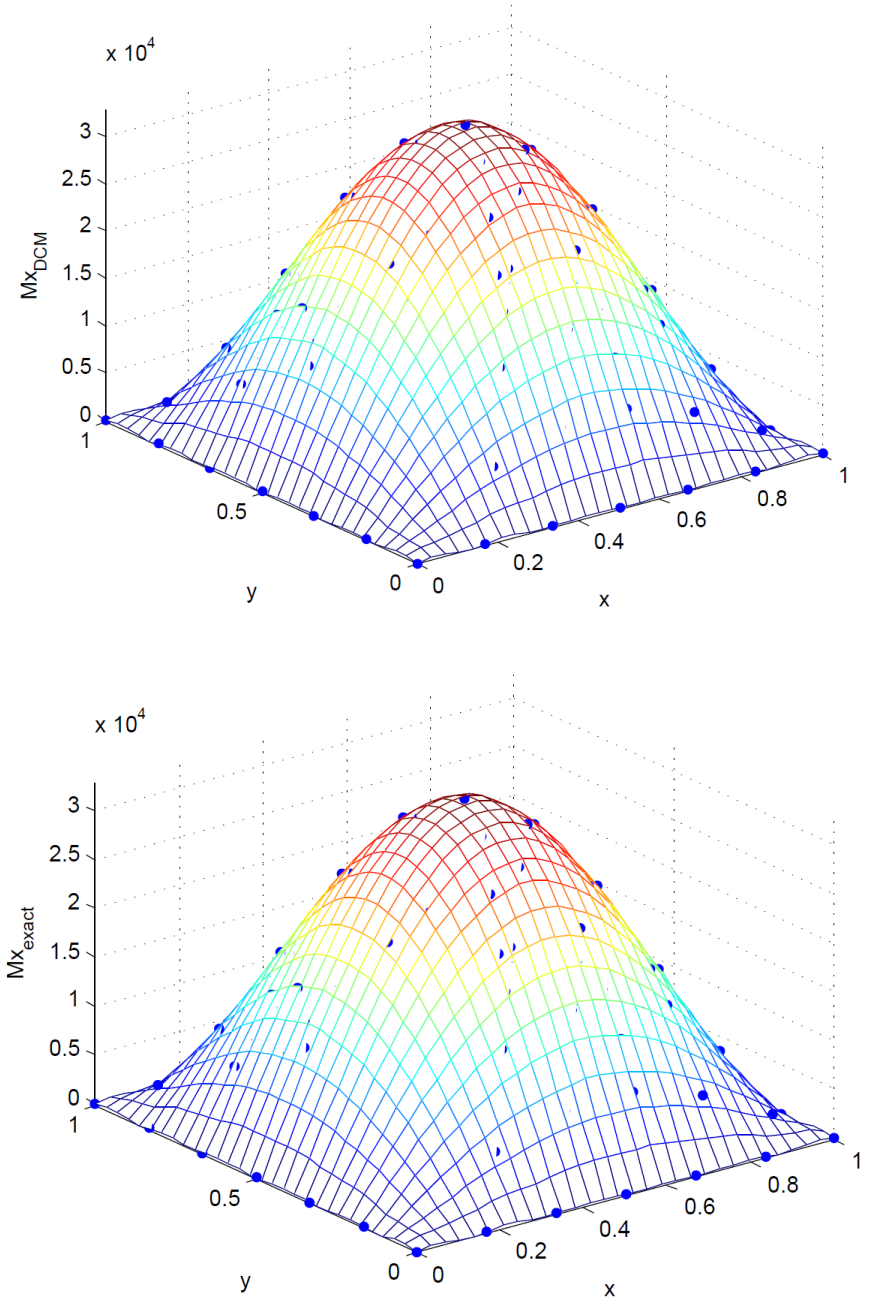

Figure 8. Numerical (top) and analytical (bottom) results for M_x in a simply supported plate (SSSS).

eral, affects numerical computations and hence warrants further theoretical and numerical studies.

Acknowledgments

The second author has been supported by Academy of Finland through the project *Adaptive Isogeometric methods for thin-walled structures* (decision number 270007). The third author has been supported by Academy of Finland through the project *How to handle the prima donna of structures: analysis and development of advanced discretization techniques for the simulation of thin shells* (decision number 260302).

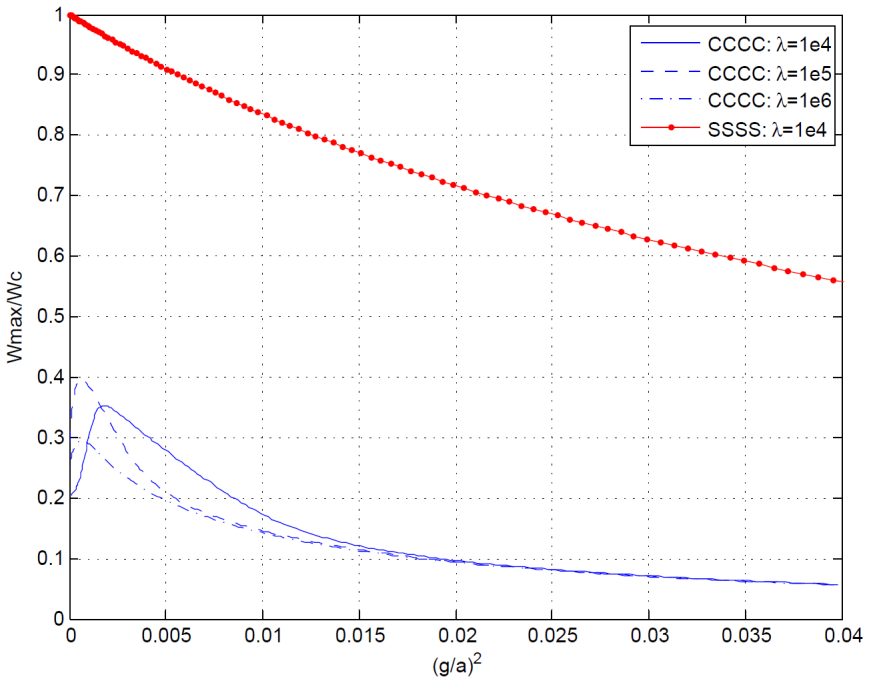

Figure 9. The normalized central deflection versus gradient parameter (SSSS, CCCC), $n = 85$.

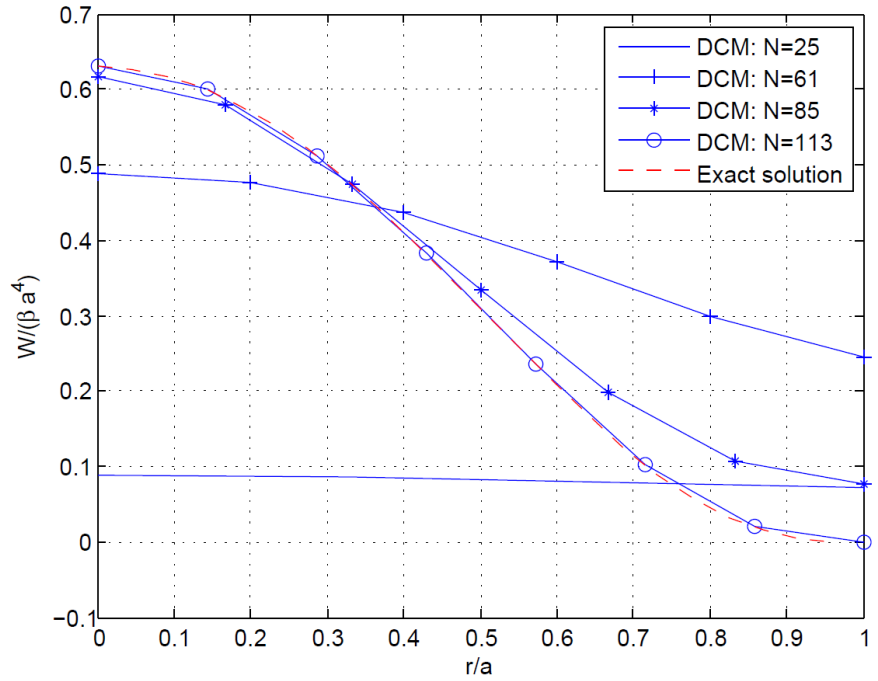

Figure 10. The normalized radial deflection of the circular plate with clamped boundary, $g = 0.1a$, $\lambda = 1e4$ and $\beta = q_0/(64D)$.

References

[1] A. R. Ahmadi and Hamed Farahmand. Static deflection analysis of flexural rectangular micro-plate using higher continuity finite-element method. *Mechanics and Industry*, 13:261–269, 2012. doi:10.1051/meca/2012019.

[2] A. R. Ahmadi, Hamed Farahmand, and S. Arabnejad. Static deflection analysis of flexural simply supported sectorial micro-plate using p-version finite-element method. *Int J Multiscale Comput Eng*, 9:193–200, 2011. doi:10.1615/IntJMultCompEng.v9.i2.40.

[3] H. Altenbach, G.A. Maugin, and V. Erofeev. *Mechanics of Generalized Continua, Series: Advanced Structured Materials*, volume 7. Springer-Verlag, Berlin Heidelberg, 2011.

[4] D. N. Arnold, A. L. Madureira, and S. Zhang. On the range of applicability of the Reissner–Mindlin and Kirchhoff–Love plate bending models. *J. Elasticity*, 67: 171–185, 2002.

[5] J.-L. Batoz, K.-J. Bathe, and L. W. Ho. A study of three-node triangular plate bending elements. *Int. J. Num. Meths. Eng.*, 15:1771–1812, 1980. doi:10.1002/nme.1620151205.

[6] J. L. Batoz, C. L. Zheng, and F. Hammadi. Formulation and evaluation of new triangular, quadrilateral, pentagonal and hexagonal discrete Kirchhoff plate/shell elements. *Int. J. Num. Meths. Eng.*, 52:615–630, 2001. doi:10.1002/nme.295.

[7] E. M. Behrens and J. Guzman. A mixed method for the biharmonic problem based on a system of first-order equations. *SIAM J. Num. Anal.*, 49:789–817, 2011. doi:10.1137/090775245.

[8] L. Beirão da Veiga, J. Niiranen, and R. Stenberg. A family of C^0 finite elements for Kirchhoff plates I: Error analysis. *SIAM J. Num. Anal.*, 45:2047–2071, 2007. doi:10.1137/06067554X.

[9] L. Beirão da Veiga, J. Niiranen, and R. Stenberg. A family of C^0 finite elements for Kirchhoff plates II: Numerical results. *Comp. Meths. Appl. Mech. Engrg.*, 197: 1850–1864, 2008. doi:10.1016/j.cma.2007.11.015.

[10] S. P. Beskou and D. E. Beskos. Static, stability and dynamic analysis of gradient elastic flexural Kirchhoff plates. *Arch Appl Mech*, 78:625–635, 2008.

[11] S. P. Beskou, A.E. Giannakopoulos, and D.E. Beskos. Variational analysis of gradient elastic flexural plates under static loading. *Int J Solids Struct*, 47:2755–2766, 2010. doi:10.1016/j.ijsolstr.2010.06.003.

[12] W. Chen and T. Zhong. The study on the nonlinear computations of the dq and dc methods. *Num Meth Part Diff Eq*, 13:57–75, 1997. doi:10.1002/(SICI)1098-2426(199701)13:1<57::AID-NUM5>3.0.CO;2-L.

[13] P. G. Ciarlet. *Mathematical Elasticity – Volume II: Theory of Plates*. Elsevier, Amsterdam, 1997.

[14] F. Civan. Solving multivariable mathematical models by the quadrature and cubature methods. *Numer. Meth. Partial Differential Eq.*, 10:545–567, 1994. doi:10.1002/num.1690100503.

[15] P. Destuynder. Explicit error bounds for the Kirchhoff–Love and Reissner–Mindlin plate models. *C. R. Acad. Sci. Series I*, 325:233–238, 1997.

[16] P. Destuynder and T. Nevers. A new finite element scheme for bending plates. *Comp. Meths. Appl. Mech. Engrg.*, 68:127–139, 1988. doi:10.1016/0045-7825(88)90111-9.

[17] P. Destuynder and M. Salaun. *Mathematical Analysis of Thin Plate Models*. Springer-Verlag, Berlin, 1996.

[18] G. Engel, K. Garikipati, T. J. R. Hughes, M. G. Larson, L. Mazzei, and R. L. Taylor. Continuous/discontinuous finite element approximations of fourth-order elliptic problems in structural and continuum mechanics with applications to thin beams and plates, and strain gradient elasticity. *Comp. Meths. Appl. Mech. Engrg.*, 191: 3669–3750, 2002. doi:10.1016/S0045-7825(02)00286-4.

[19] K. Jongkittinarukorn F. Escobar and F. Civan. Cubature solution of the poisson equation. *Communications in Numerical Methods in Engineering*, 13:453–465, 1997. doi:10.1002/(SICI)1099-0887(199706)13:6<453::AID-CNM72>3.0.CO;2-O.

[20] D.C.C. Lam, F. Yang, A.C.M. Chong, J. Wang, and P. Tong. Experiments and theory in strain gradient elasticity. *J Mech Phys Solids*, 51:1477–1508, 2003. doi:10.1016/S0022-5096(03)00053-X.

[21] K.A. Lazopoulos. On bending of strain gradient elastic micro-plates. *Mech Res Commun*, 36:777–783, 2009. doi:10.1016/j.mechrescom.2009.05.005.

[22] K. M. Liew and F. L. Liu. Differential cubature method: a solution technique for kirchhoff plates of arbitrary shape. *Comput. Methods Appl. Mech. Eng.*, 145:1–10, 1997. doi:10.1016/S0045-7825(96)01194-2.

[23] F. L. Liu and K. M. Liew. Differential cubature method for static solutions of arbitrarily shaped thick plates. *Int. J. Solids Struct.*, 35:3655–3674, 1998. doi:10.1016/S0020-7683(97)00215-1.

[24] R. Maranganti and P. Sharma. A novel atomistic approach to determine strain-gradient elasticity constants: Tabulation and comparison for various metals, semiconductors, silica, polymers and the (ir) relevance for nanotechnologies. *J Mech Phys Solids*, 55:1823–1852, 2007. doi:10.1016/j.jmps.2007.02.011.

[25] L. S. D. Morley. The triangular equilibrium element in the solution of plate bending problems. *Aero. Quart.*, 19:149–169, 1968.

[26] S. M. Mousavi. Differential cubature method for static solution of laminated shells of revolution with mixed boundary conditions. *Key Eng Mater*, 471:1005–1009, 2011. doi:10.4028/www.scientific.net/KEM.471-472.1005.

[27] S. M. Mousavi and M.M. Aghdam. Static bending analysis of laminated cylindrical panels with various boundary conditions using the differential cubature method. *J Mech Mater Struct*, 4:509–521, 2009. doi:10.2140/jomms.2009.4.509.

[28] S. M. Mousavi and J. Paavola. Analysis of plate in second strain gradient elasticity. *Arch Appl Mech*, 84:1135–1143, 2014. doi:10.1007/s00419-014-0871-9.

[29] S. M. Mousavi, J. Paavola, and J.N. Reddy. Variational approach to dynamic analysis of third-order shear deformable plates within gradient elasticity. *Meccanica*, 50:1537–1550, 2015. doi:10.1007/s11012-015-0105-4.

[30] A. Ashoori Movassagh and M.J. Mahmoodi. A micro-scale modeling of Kirchhoff plate based on modified strain-gradient elasticity theory. *Eur. J. Mech. A/Solids*, 40: 50–59, 2013. doi:10.1016/j.euromechsol.2012.12.008.

[31] C. Schwab. A-posteriori modeling error estimation for hierarchic plate models. *Numer. Math.*, 74:221–259, 1996.

[32] C. Schwab and S. Wright. Boundary layers of hierarchical beam and plate models. *J. Elasticity*, 38:1–40, 1995.

[33] T. M. Teo and K. M. Liew. Differential cubature method for analysis of shear deformable rectangular plates on pasternak foundations. *Int. J. Mech. Sci.*, 44:1179–1194, 2002. doi:10.1016/S0020-7403(02)00034-6.

[34] K. G. Tsepoura and D. Polyzos. Static and harmonic bem solutions of gradient elasticity problems with axisymmetry. *Comput Mech*, 32:89–103, 2003. doi:10.1007/s00466-003-0464-x.

[35] G.C. Tsiatas. A new Kirchhoff plate model based on a modified couple stress theory. *Int J Solids Struct*, 46:2757–2764, 2009. doi:10.1016/j.ijsolstr.2009.03.004.

[36] S.V. Tsinopoulos, D. Polyzos, and D.E. Beskos. Static and dynamic bem analysis of strain gradient elastic solids and structures. *Comput Model Eng Sci*, 86:113–144, 2012.

[37] B. Wang, S. Zhou, J. Zhao, and X. Chen. A size-dependent Kirchhoff micro-plate model based on strain gradient elasticity theory. *Eur. J. Mech. A/Solids*, 30:517–524, 2011. doi:10.1016/j.euromechsol.2011.04.001.

[38] X. Wang and F. Wang. Size-dependent dynamic behavior of a microcantilever plate. *J Nanomat*, 2012, 2012. doi:10.1155/2012/891347.

[39] L. Wu and J. Liu. Free vibration analysis of arbitrary shaped thick plates by differential cubature method. *Int. J. Mech. Sci.*, 47:63–81, 2005. doi:10.1016/j.ijmecsci.2004.12.003.

[40] S. Tahaei Yaghoubi, S. M. Mousavi, J. Paavola, and J.N. Reddy. Strain and velocity gradient theory for higher-order shear deformable beams. *Arch Appl Mech*, 85:877–892, 2015. doi:10.1007/s00419-015-0997-4.

[41] S. Zhang. On the accuracy of Reissner–Mindlin plate model for stress boundary conditions. *ESAIM Math. Mod. Numer. Anal.*, 40:269–294, 2006. doi:10.1051/m2an:2006014.

S. Mahmoud Mousavi, Jarkko Niiranen, Antti H. Niemi
Department of Civil and Structural Engineering,
Aalto University School of Engineering,
P.O. Box 12100, 00076 AALTO, Finland
mahmoud.mousavi@aalto.fi, jarkko.niiranen@aalto.fi, antti.h.niemi@aalto.fi